EDGEWOOD

CHEMICAL BIOLOGICAL CENTER

U.S. ARMY RESEARCH, DEVELOPMENT AND ENGINEERING COMMAND

ECBC-TR-447

RELATIONSHIPS AND TRANSFORMATIONS BETWEEN CONCENTRATION-PATH-LENGTH (*CL*), AGENTS CONTAINING PARTICLES PER LITER OF AIR (*ACPLA*), AND THE NUMBER OF SPORES (N_{spores})

Avishai Ben-David
Alan C. Samuels
Ronny C. Robbins
James O. Jensen

RESEARCH AND TECHNOLOGY DIRECTORATE

November 2005

ABERDEEN PROVING GROUND, MD 21010-5424

Disclaimer

The findings in this report are not to be construed as an official Department of the Army position unless so designated by other authorizing documents.

REPORT DOCUMENTATION PAGE

Form Approved
OMB No. 0704-0188

1. REPORT DATE *(DD-MM-YYYY)*	2. REPORT TYPE	3. DATES COVERED *(From - To)*
XX-11-2005	Final	Jan 2004 – Dec 2004

4. TITLE AND SUBTITLE
Relationships and Transformations between Concentration-path-Length (*CL*), Agents Containing Particles per Liter of Air (*ACPLA*), and the Number of Spores (N_{spores})

5a. CONTRACT NUMBER

5b. GRANT NUMBER

5c. PROGRAM ELEMENT NUMBER

6. AUTHOR(S)
Ben-David, Avishai; Samuels, Alan C.; Robbins, Ronny C.; and Jensen, James O. (ECBC)

5d. PROJECT NUMBER
None

5e. TASK NUMBER

5f. WORK UNIT NUMBER

7. PERFORMING ORGANIZATION NAME(S) AND ADDRESS(ES)
DIR, ECBC, ATTN: AMSRD-ECB-PT-DP//AMSRD-ECB-RT-DD, APG, MD 21010-5424

8. PERFORMING ORGANIZATION REPORT NUMBER
ECBC-TR-447

9. SPONSORING / MONITORING AGENCY NAME(S) AND ADDRESS(ES)

10. SPONSOR/MONITOR'S ACRONYM(S)

11. SPONSOR/MONITOR'S REPORT NUMBER(S)

12. DISTRIBUTION / AVAILABILITY STATEMENT
Approved for public release; distribution is unlimited.

13. SUPPLEMENTARY NOTES
Presented at the 6th Joint Conference on Standoff Detection for Chemical and Biological Defense, October 25-29, 2004, Williamsburg, VA

14. ABSTRACT
Threat levels and detection objectives are usually given as Agent-Containing-Particles per Liter of Air (*ACPLA*) where agents can be taken as spores (microbes, toxins, viruses) that are "stuck" together to form an aggregate (super) particle characterized by size distribution and the packing efficiency of the agents. The number of agents (spores), N_{spores}, in *ACPLA* is of interest for assessing the pathogenic level of the threat. Most standoff sensors measure mass-column-density (Concentration-path-Length) *CL* that is the integrated mass of the spores along the detection path-Length. This study explores the relationships between *ACPLA*, N_{spores}, and *CL* and outlines a computational procedure with examples of different types of bacteria and spores.

15. SUBJECT TERMS

ACPLA	Spores	Bacteria	*Bacillus subtilus*	Concentration-path-Length
CL	Bioaerosols	Aerosol size distribution	Standoff Detection	N_{spores}

16. SECURITY CLASSIFICATION OF:			17. LIMITATION OF ABSTRACT	18. NUMBER OF PAGES	19a. NAME OF RESPONSIBLE PERSON
a. REPORT	b. ABSTRACT	c. THIS PAGE			Sandra J. Johnson
U	U	U	UL	32	19b. TELEPHONE NUMBER *(include area code)* 410-436-2914

Blank

PREFACE

The work described in this report was started in January 2004 and completed in December 2004.

The use of either trade or manufacturers' names in this report does not constitute an official endorsement of any commercial products. This report may not be cited for purposes of advertisement.

This report has been approved for public release. Registered users should request additional copies from the Defense Technical Information Center; unregistered users should direct such requests to the National Technical Information Service.

Blank

CONTENTS

FIGURES

TABLES

Blank

RELATIONSHIPS AND TRANSFORMATIONS BETWEEN CONCENTRATION-PATH-LENGTH (*CL*), AGENTS CONTAINING PARTICLES PER LITER OF AIR (*ACPLA*), AND THE NUMBER OF SPORES (N_{spores})

1. INTRODUCTION

In remote sensing, passive Infrared (IR) sensors (e.g., Fourier-transform, FTIR spectrometers), measure mass-column-density (Concentration-path-Length (CL) mg/m^2). Aerosol mass concentration is represented by C (mg/m^2) and L (m) is the path-Length along the line-of-sight of the sensor containing the aerosols. The threat level (detection objective) is usually alluded to as Agent-Containing-Particles per Liter of Air (*ACPLA*). Agents can be either spores (microbes, toxins, viruses) that are "stuck" together to form an aggregate *ACPLA* particle or the spores can be cohered to the surface of a large particle such as dust. The quantities of interest are listed below:

(a) The CL (the cumulative mass of the spores along a detection path-Length).
(b) The number of spores (N_{spores}) along a path-Length.
(c) The *ACPLA* (the number of aggregates in a liter of air).

The 3 concepts, CL , N_{spores} , and *ACPLA,* are of interest to different members of the community for different reasons. For the engineer who builds an IR sensor, CL and, therefore, N_{spores} and their cumulative mass, are crucial parameters for determining the sensitivity of the sensor. The relationship between N_{spores} and CL is also useful for computing fluorescent cross-sections from bioaerosols. For the person who designs and evaluates the efficiency of delivery systems, *ACPLA* is of interest. A sensor based on counting particles by light scattered from a particle also uses *ACPLA*. For a physician, the concept of N_{spores} is critical.

This study explores the relationship between CL , N_{spores} , and *ACPLA* , and illustrates a computational procedure that transforms *ACPLA* to CL and N_{spores} . The difference between *ACPLA* and *CL* is determined by the spore count in an aggregate of a certain size, which is dependent on bacteria type and the dissemination scenario for the spores, which, in turn, gives rise to the issue of packing density.

2. NUMBER AND SIZE VOLUME DISTRIBUTION

The aerosol number size distribution density function, $f_n(r)$, is modeled as a lognormal distribution. In the context of this study, $f_n(r)$ will be regarded as the size distribution of the aggregate of size (r). For convenience, (r) will be regarded as the "radius" of a spherical aggregate. The aerosol number size distribution density is given as

$$f_n(r:\mu,\sigma)=\frac{1}{r\sqrt{2\pi(\ln\sigma)^2}}\exp[-\frac{(\ln r-\ln\mu)^2}{2(\ln\sigma)^2}] \qquad (1)$$

$$N=\int f_n(r:\mu,\sigma)dr \quad (\textit{number of aerosol particles within a unit volume})$$

where μ and σ are the parameters of the log-normal size distribution; $f_n(r)dr$ is the number of aerosols within radii $r\pm\frac{dr}{2}$; and N is the total number of aerosol particles in a unit of volume. When the unit of volume is taken as 1 *liter*, $ACPLA = N\ (liter^{-1})$.
The equation for volume size distribution density function, $f_v(r)$, is given as

$$f_v(r:\mu,\sigma)=f_n(r:\mu,\sigma)\frac{4\pi r^3}{3} \qquad (2)$$

where $f_v(r)dr$ is the volume of aerosol particles of radius $r\pm\frac{dr}{2}$. The total volume is $V(\mu,\sigma)$. Equation 2 and all aerosol radii sizes are integrated to determine V and the CL:

$$V(\mu,\sigma)=\int_{r_{min}}^{r_{max}}\frac{4\pi r^3}{3}f_n(r)dr=\int_{r_{min}}^{r_{max}}\frac{4\pi r^3}{3}\frac{1}{r\sqrt{2\pi(\ln\sigma)^2}}\exp[-\frac{[\ln r-\ln\mu]^2}{2(\ln\sigma)^2}]dr=\int_{r_{min}}^{r_{max}}f_v(r)dr \qquad (3)$$

3. PARAMETERS FOR NUMBER DENSITY $f_n(r)$ AND VOLUME DENSITY $f_v(r)$ DISTRIBUTIONS

The parameters that describe the lognormal distribution $f(r:\mu,\sigma)$ are *mode radius* (r_{mode}), *median radius* (r_{median}), *mean radius* (r_{mean}), and *standard deviation* (*std* of the distribution). All 4 parameters are a function of 2 variables (μ,σ) that characterize the lognormal distribution given in eq 1. The r_{mode} is used when size distribution is at its peak: $f(r=r_{mode})=\max$. For r_{median}, defined as $\int_{r\,median}^{\infty}f(r)dr=0.5$, 50% of the distribution area is above the radius. The r_{mean} parameter is defined as $r_{mean}=\int_0^{\infty}rf(r)dr$ (the first moment of the distribution). The *std* of the distribution is defined as $std=\sqrt{\int_0^{\infty}(r-r_{mean})^2f(r)dr}$ with a lognormal distribution, $std\neq\sigma$. While r_{mean}, r_{median} and *std* are all functions of the integration limits $[r_{min},r_{max}]$, which are implicitly 0 and

∞ in eqs 4 and 5, r_{mode} does not depend on the radii range $[r_{min}, r_{max}]$ used in the size distribution function, $f(r)$.

For the number density size distribution $f_n(r:\mu,\sigma)$, where the radii (r) is unbounded (0 to ∞), the parameters are

$$\left\{\begin{array}{l} r_{mean} = \exp(\ln\mu + 0.5(\ln\sigma)^2) \\ r_{mode} = \exp(\ln\mu - (\ln\sigma)^2) \\ r_{median} = \mu \\ std = \sqrt{\exp[2\ln\mu + (\ln\sigma)^2][\exp((\ln\sigma)^2) - 1]} \end{array}\right\} \quad (4)$$

For the volume density function $f_v(r:\mu,\sigma)$, the parameters are

$$\left\{\begin{array}{l} r_{mean} = \exp[t + 0.5(\ln\sigma)^2] \\ r_{mode} = \exp[t - (\ln\sigma)^2] \\ r_{median} = \exp(t) \\ std = \sqrt{\exp[2t + (\ln\sigma)^2][\exp((\ln\sigma)^2) - 1]} \\ where\ t = \ln\mu + 3(\ln\sigma)^2 \end{array}\right\} \quad (5)$$

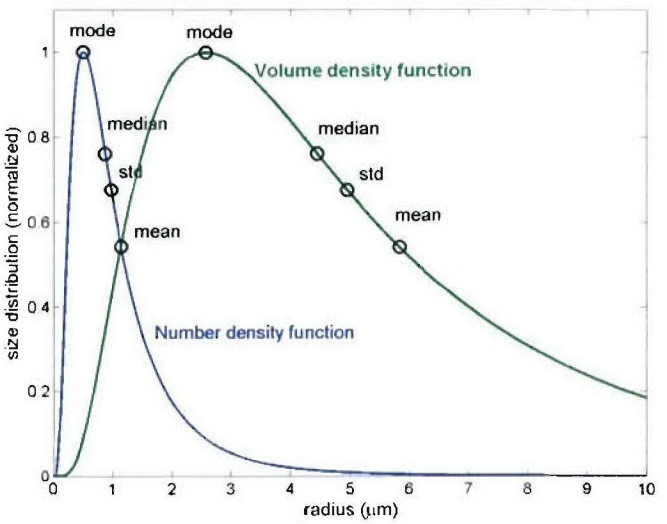

Figure 1a. Number and Volume Density Lognormal Distributions for a Typical Bioaerosol (μ = 0.875 μm, σ = 2.09 μm).

In Figure 1a, number and volume density lognormal distributions are shown for typical bioaerosol parameters. For the number density distribution, $f_n(r)$, the parameters are

$r_{mode} = 0.5\mu m$,
$r_{median} = 0.87\mu m$,
$r_{mean} = 1.14\mu m$, and
$std = 0.97\mu m$.

For the volume density distribution, $f_v(r)$, the parameters are

$r_{mode} = 2.58\mu m$,
$r_{median} = 4.44\mu m$,
$r_{mean} = 5.83\mu m$, and
$std = 4.95\mu m$.

For both Figures 1a and 1b, the parameters for the r_{median}, *std,* and r_{mean}, which are dependent on the value of r_{max}, are for size distribution with radii $0 < r < (r_{max} \to \infty)$. The location for r_{mode} is independent of r_{max}.

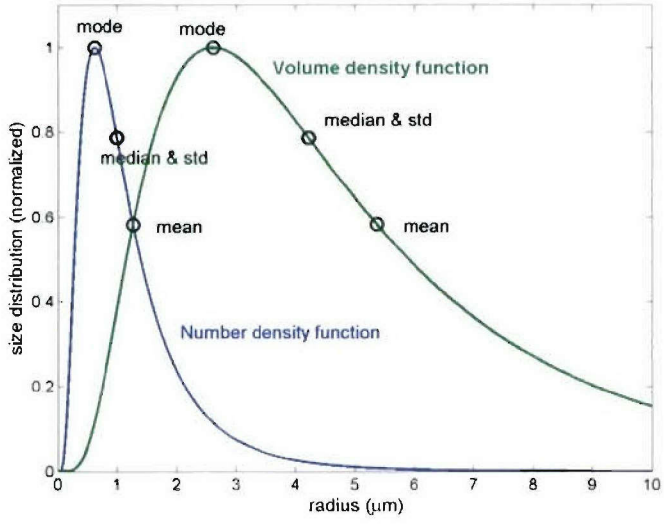

Figure 1b. Number Density $f_n(r: \mu, \sigma)$ and Volume Density $f_v(r: \mu, \sigma)$ Lognormal Distributions ($\mu = 1\ \mu m$, $\sigma = 2\ \mu m$).

The lognormal distributions for number density, $f_n(r:\mu,\sigma)$, and volume density, $f_v(r:\mu,\sigma)$, are illustrated in Figure 1b. For convenience, this size distribution was used to represent bioaerosol throughout the examples given in this study (Figures 1a and1b are very similar). The parameters for the number density distribution, $f_n(r)$, are

$r_{mode} = 0.62\mu m$,
$r_{median} = 1\mu m$,
$r_{mean} = 1.27\mu m$, and
$std = 0.99\mu m$.

The parameters for the volume density distribution $f_v(r)$ are

$r_{mode} = 2.61\mu m$,
$r_{median} = 4.23\mu m$,
$r_{mean} = 5.37\mu m$, and
$std = 4.22\mu m$.

Due to gravitational settling, some particles fall to the ground while traveling a distance (x) with a wind velocity (u) within the time frame ($t=x/u$). The falling particles can also be subjected to other deposition processes such as turbulence to a non-reflecting surface and rain.[1] When a particle of radius (r) is dropped from a height (H), the falling velocity will at first increase (acceleration by gravity) and then, after a time (t) and a distance (h) (due to the drag force), the particle will reach a terminal settling velocity for the remaining distance to the ground.

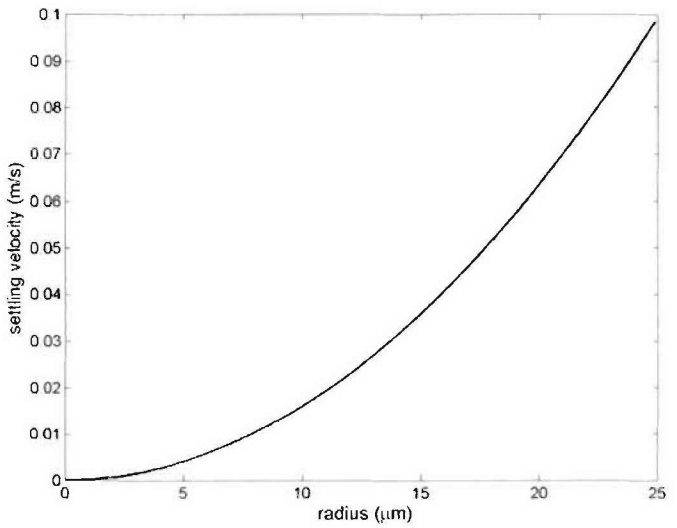

Figure 2. Terminal Settling Velocity of Sphere.

Figure 2 portrays the terminal velocity of a particle of radius (r) and density of $\rho = 1.32\ g\,cm^{-3}$ falling in still air at 20 ^{o}C temperature. The time taken for reaching terminal velocity is less than 0.01 s. A particle with a radius of 25 μm, dropped from a height of 100 m and carried out by a wind at a velocity of 3 m/s (~10 km/hr), will travel a distance of 3 km before it hits the ground. Thus, great care is needed in choosing the maximum radius in a given aerosol size distribution for a particular scenario.

4. TOTAL VOLUME AND UPPER-LIMIT *CL* ESTIMATE FOR AEROSOL SIZE DISTRIBUTION

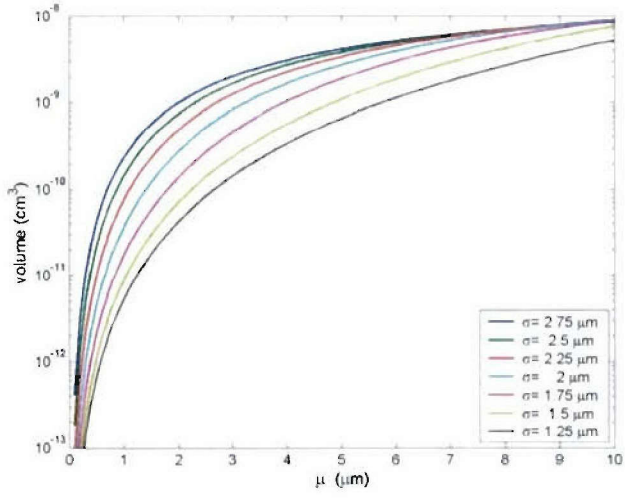

Figure 3. Total Volume $V(\mu, \sigma)$ of All Particles in Lognormal Number Density Distribution $f_n(r: \mu, \sigma)$.

In Figure 3, the total volume, $V(\mu,\sigma)$, as discussed in eq 3, of all the particles is shown in the lognormal number density distribution, $f_n(r:\mu,\sigma)$. The total number of particles (N), in $f_n(r)$, within a unit volume is assumed to be $N = \int_{r_{\min}}^{r_{\max}} f_n(r)dr = 1$. The range of particle radii is between $r_{\min} \to 0$ and $r_{\max} = 25\mu m$. When the unit of volume is taken to be 1 *liter*, $ACPLA = N\ (liter^{-1})$.

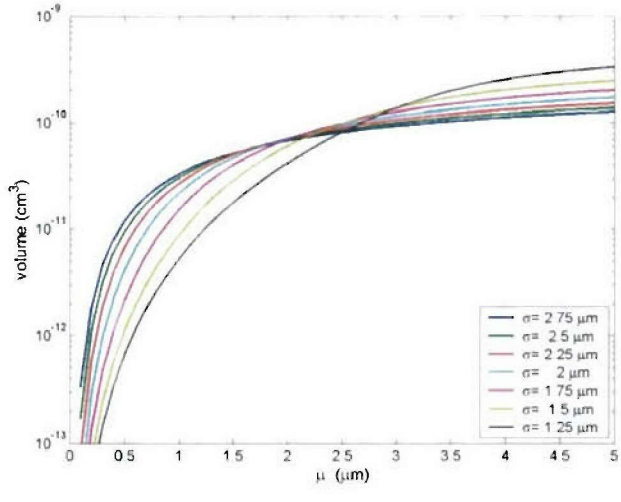

Figure 4. Same as Figure 3, but the Largest Radius ($r_{\max} = 5\mu m$) Shows Only Small Particles Being of Interest.

Figure 4 also shows total volume $V(\mu,\sigma)$. The largest radius ($r_{\max} = 5\mu m$) reflects a scenario in which only small particles are of interest. Some of the curves are shown to cross each other around $\mu \sim 2.5\mu m$. This seemingly strange behavior is ascribed to the fact that for each pair of (μ,σ), the total number of particles (N) in $f_n(r)$ is the same. The median and mode of the distribution is a function of (μ,σ). As the value of (μ,σ) increases, most particles (mode of distribution) shift toward a larger radius: for $\mu \sim 2.5\mu m$ and $\sigma > 1.75\mu m$, r_{mode} shifts to $r > 5\mu m$. However, due to the constraint of $r_{\max} = 5\mu m$ in the size distribution, particles with $r > 5\mu m$ (the expected mode of distribution) cannot be attained. Thus, the increase in overall volume is possible only by the small particles with $r < 5\mu m$ whose relative number is a function of (μ,σ). The rate of increase for curves with smaller σ is faster due to the fact that the mode of distribution has not yet been reached.

The conversion of total volume (V) (the *y-axis* of Figures 3 and 4) to *CL* is straightforward. The unit volume assumed for the total number of particles (N) in $f_n(r)$ can be taken to be 1 *liter* (1000 cm^3). Thus, for a given aerosol density, ρ ($\frac{g}{cm^3}$) and a path-Length of L (m), the Concentration-path-Length product (mass-column-density, *CL*) is

$$CL\,(\frac{mg}{m^2}) = N\frac{particles}{liter}\times 10^3\frac{liters}{m^3}V(cm^3)\times\rho(\frac{g}{cm^3})\times 10^3\frac{mg}{g}\times L(m) \qquad (6)$$

The *CL* in eq 6 symbolizes the aerosol material (ρ) in the size distribution $f_n(r:\mu,\sigma)$. Not all the aerosol mass in $f_n(r:\mu,\sigma)$ consists of the desired agent material (*BG spores*) because of the packing efficiency (the fractional volume of the spores within the aerosols) of the spores into aggregate "particles". Thus, the computed *CL* value in eq 6 may be regarded as an upper-limit estimate whereas the correct *CL* will be much lower when the volume occupied by the spores in the aggregate is accounted for (Section 8).

The N_{spores} present in the given size distribution, $f_n(r)$, is obtained by calculating for *CL*. For 1000 *ACPLA*, a 100-meter path-Length and a size distribution $f_n(r:\mu=1,\sigma=2)$ (Fig. 1b) with (*BG*) a density of $\rho = 1.32\ g/cm^3$, the (upper-limit) estimate for *CL* derived with eq 6 is

$$CL = 1000(\frac{particle}{liter})\times 4\times 10^{-11}\,(cm^3)\times 1.32\,(g/cm^3)\times 100(m)\times 10^6 = 5.3\,\frac{mg}{m^2}$$

for particles with $r < 25\mu m$ (Figure 3). When only small particles with $r < 5\mu m$ (Figure 4) are considered, *CL* will be calculated as

$$CL = 1000(\frac{particle}{liter}) \times 2 \times 10^{-11}\,(cm^3) \times 1.32\,(g/cm^3) \times 100(m) \times 10^6 = 2.6\,\frac{mg}{m^2}.$$

Density of *Bacillus subtilis BG* spores.

Only a few references to the density of *Bacillus subtilis BG* spores are available for light and heavy spores: 1.45 g/cm^3,[2] 1.2 g/cm^3,[3] 1.290 g/cm^3, and 1.335 g/cm^3.[2-5] The difference between the values may partly be a result of the amount of water in a *BG* particle. Apparently, no "hard numbers," which are extremely important for estimating mass-column-density *CL,* exist for *BG* density. In this study, the average of all the reported densities was taken to attain the value of 1.32 g/cm^3.

5. PHYSICAL DESCRIPTION AND PROPERTIES OF BACTERIA AND SPORES

Typical members of several bacterial species are shown in Figure 5.[5] Each of the first top 3 bacteria is represented by a single spore. The last 3 bacteria, the bacterium being the spore, are taken to be single-celled organisms. The bacteria, modeled in a super-ellipsoid as *x-y-z* coordinates, are given as

$$(\frac{x}{a})^n + (\frac{y}{b})^n + (\frac{z}{c})^n = 1 \qquad (7)$$

The semi-axes of the ellipsoid are *a*, *b* and *c*. When $a = b < c$ and $n = 2$, eq 7 describes the regular prolate and when $a = b = c$, $n = 2$, eq 7 is a sphere with radius *a*.

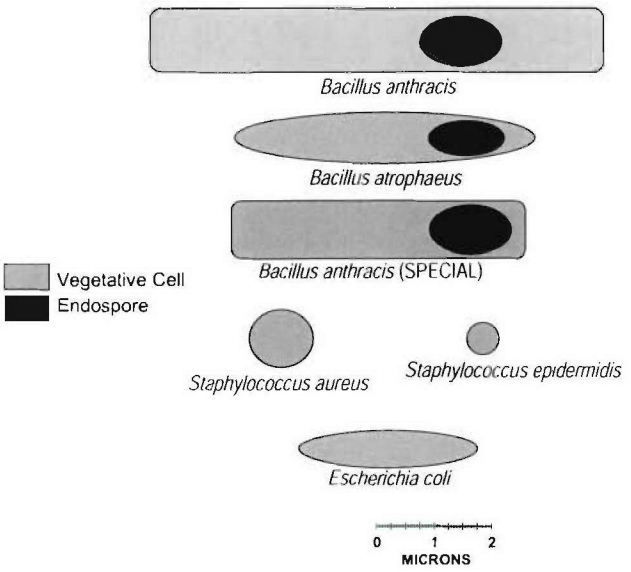

Figure 5. Typical Members of Several Bacterial Species[5] where, for the First Top 3 Bacteria, a Single Spore is Inserted. The last 3 bacteria are taken to be single-celled organisms (the bacterium is the spore).

The volume of the super-spheroid is calculated as

$$V = \frac{8abc}{n^2}\beta(\frac{1}{n}+1,\frac{2}{n})\beta(\frac{1}{n},\frac{1}{n}) \tag{8}$$

The mathematical beta function is $\beta(z,w) = \int_0^1 t^{z-1}(1-t)^{w-1}\,dt$ and the volume equation [6] has been modified for eq 7.[5]

Table 1 contains physical parameters for the bacteria and spores. Additional reports on elliptically shaped (~1 μm long and ~0.7 μm wide)[5] *Bacillus subtilis BG* spores[7-9] and rod-shaped (~0.5 μm wide and 1-2 μm long) *Erwinia herbicola*[10-12] are in existence. Estimating the N_{spores} is crucial for estimating the *CL* that can be contained in a particle of radius (r). This issue is addressed in 2 different ways in Sections 6 and 8.

Table 1. Physical Properties of Selected Bacteria and Spores.

	Bacillus subtilis (superspheroid)		*Bacillus anthracis* (superspheroid)		*Bacillus anthracis* (superspheroid, SPECIAL case)		*Staphylococus aureus* (sphere)	*Staphylococus epidermidis* (sphere)	*Escherichia coli* (rod)	*Erwinia herbicola* (rod)
	bacteria	spore	bacteria	spore	bacteria	spore	bacteria	bacteria	bacteria	bacteria
a (μm)	0.38	0.33	0.6	0.45	0.5	0.45	0.5	0.3	0.27	0.25
b (μm)	0.38	0.33	0.6	0.45	0.5	0.45	0.5	0.3	0.27	0.25
c (μm)	2.5	0.6	4	0.7	2.5	0.7	0.5	0.3	1.5	1.5
n	3.5	2	8	2	6	2	2	2	2	1.56
$V(\mu m^3)$ (Eq. 8)	2.22	0.27	10.82	0.59	4.50	0.59	0.52	0.11	0.46	0.15
mass (10^{-12} g) for assumed density $\rho = 1.32\ g\ cm^{-3}$	2.93	0.356	14.282	0.779	5.94	0.779	0.686	0.145	0.607	0.198
aspect ratio $\eta = \frac{c}{a}$	6.58	1.82	6.66	1.55	5	1.55	1	1	5.55	6
packing efficiency Φ (Eq. 10)	0.306	0.406	0.305	0.406	0.337	0.406	0.385	0.385	0.326	0.317
radius (μm) of *equivalent – volume* sphere	0.81	0.40	1.37	0.52	1.02	0.52	0.50	0.30	0.48	0.33

Erwinia herbicola: rod with width 0.5 μm and length 1 μm to 2 μm where the parameters a,b,c,n were fit to match the volume.[12]

Escherichia coli: rod with width 0.4 μm to 0.7 μm and length 1 to 4 μm where a,b,c,n are given by Wyatt.

All other bacteria and spores are from Wyatt.[5]

6. N_{spores} AND *CL* ESTIMATE VIA A "RULE OF THUMB"

A widely used rule of thumb propounds that the number of spores contained in a particle (aggregate) of radius (r in microns) is $(2r)^{2.55}$. This rule also states that a particle with r <0.5 μm cannot contain a spore and a particle with r = 0.5 μm is a single organism (spore). For the lognormal number size distribution $f_n(r:\mu,\sigma)$, the total N_{spores} within a unit volume and the *CL* are calculated as

$$\left\{\begin{array}{ll} N_{spores} = N\int_{0.5\mu m}^{r_{max}} (2r)^{2.55} f_n(r:\mu,\sigma)dr & (\frac{spores}{liter}) \\ CL = (N_{spores}10^3)\times(\rho_{spore}V_{spore})\times L & (\frac{mg}{m^2}) \\ N = ACPLA = \int_{r_{min}}^{r_{max}} f_n(r:\mu,\sigma)dr & (\frac{particles}{liter}) \end{array}\right\} \quad (9)$$

where ρ_{spore} is the density and V_{spore} is the volume of a single spore (eq 8) so that $\rho_{spore}V_{spore} = m_{spore}$ is the mass (mg) of a single spore. The $N_{spores}\times 10^3$ are the number of spores within a cubic meter, $(\frac{spores}{m^3})$; and L is the path-Length (m). The integration in eq 9 is started at $r = 0.5\mu m$, which is the particle with the smallest size radius within the framework of the rule that can contain a single spore.

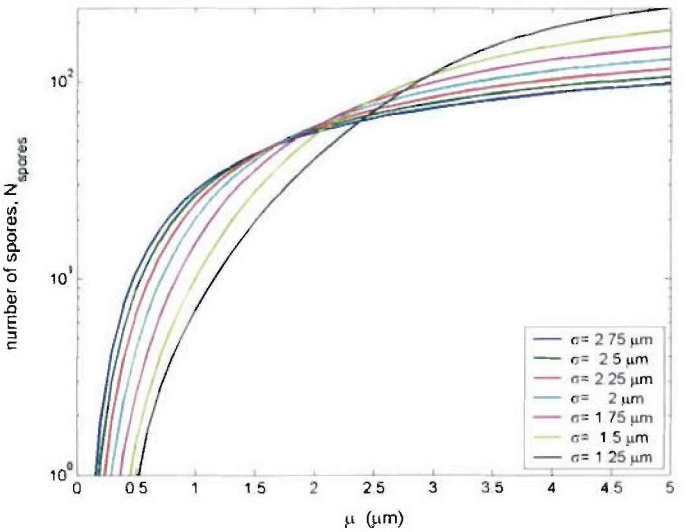

Figure 6. N_{spores} Using "Rule of Thumb" Eq 9 in the Lognormal Number Density Distribution $f_n(r:\mu,\sigma)$ with Particles = $r \geq 5\mu m$.

In Figure 6, the N_{spores} estimate for a family of lognormal number density size distribution of $f_n(r:\mu,\sigma)$ is shown with $ACPLA = 1\ liter^{-1}$. The radii range in $f_n(r:\mu,\sigma)$ is $r_{\min} \to 0$ and $r_{\max} = 25\mu m$. While $r_{\min} \to 0$ in Figure 6, N_{spores} is computed only for $r \geq 0.5\mu m$ (eq 9). Figure 13 shows that for the lognormal size distribution $f_n(r:\mu=1,\sigma=2)$ (Figure 1b), the desired value for a 1-N_{spores} particle is 20 (N = 1 particle in Figure 13). The estimated *CL* for *BG* spores for 1000 *ACPLA*, and 100 meters path-Length is given in eq 9 as

$$CL = 1000\frac{particles}{liter} \times 20\frac{\frac{spores}{liter}}{\frac{particles}{liter}} \times 10^3\frac{liters}{m^3} \times 0.356\cdot 10^{-9} mg \times 100m = 0.712\frac{mg}{m^2}$$

The particle size distribution $f_n(r:\mu=1,\sigma=2)$ contains only particles smaller than $5\mu m$ and $\rho_{spore}V_{spore} = m_{spore} = 0.356\cdot 10^{-12}\,g \times 10^3\frac{mg}{g} = 0.356\cdot 10^{-9}\,mg$ (Table 1).

The mass of the *BG* spores (0.356 10^{-12} *g*), not the mass of the *BG* bacterium (2.93 10^{-12} *g*), was chosen on the assumption that only the spore material contains spectral information for detection algorithms. The bacteria material is mainly water. Assuming both bacteria and spore density are the same (1.32 g/cm^3), the *CL* from the bacteria, 1 spore per bacterium (20 bacteria/l for *liter* particle/*liter*), is much larger due to mass ratio: $0.712 \times \frac{2.93}{0.356} = 5.86\frac{mg}{m^2}$.

7. PACKING EFFICIENCY FOR BACTERIA AND SPORES

Packing efficiency of spheres (the fraction of volume filled by spheres) is an old unresolved issue.[13] In 1611, Kepler postulated, but did not prove, that the maximum packing efficiency of spheres is $\phi_{Kepler} = \frac{\pi}{3\sqrt{2}} \cong 0.74$ ("Kepler problem"). Over 350 years later, the theory has finally been proved by N.J.A Sloan.[14] The packing of spheres, cubes, ellipsoids and cylinders in a wide array of lattices (cubical, hexagonal, tetrahedral) continues to be a current research topic and many papers are routinely published on this subject. The experimental and theoretical aspects of packing have been repeatedly addressed by mathematicians and businesses (packing medical capsules and grains).

The method of packing particles is directly related to size distribution and shape. Particles can be packed in many ways: random packing, pouring particles one by one under gravity till the system becomes congested, shaking the container, etc. The list

seems never ending; however, this study deals specifically with spheroid and rod shaped spores and particles.

The aspect ratio $\eta = \frac{length}{width}$ of particles (Table 1) and size variation play a major role in packing: "a short spherocylinder (rod) that may not fit in an interstice when oriented in a given direction may fit when the orientation is changed".[15] Packing efficiency can be studied through the interplay between the excluded volume produced by caging a particle in contact with other particles and the number of contacts required to cage a particle. Williams and Philipse qualitatively explain packing efficiency: "for [a] very short spherocylinder, the excluded volume depends only weakly on the aspect ratio as opposed to the number of contacts necessary to cage the spherocylinder. As the aspect ratio increases, more contacts are required to cage the particle requiring a higher volume fraction. [At] higher aspect ratios, the required number of contacts plateau; however, the excluded volume increases significantly and drives the volume fraction (packing efficiency) back down".[15] The packing efficiency of a long thin rod is inversely proportionate to the aspect ratio and is given as $\phi = \frac{5.1}{2\eta}$ for $\eta > 15$.

Table 1 illustrates that the aspect ratio for this study is small, $\eta < 15$. Thus, the above formula[15] seems redundant and a method developed specifically for the packing of spheroids is used.[16] For rod-shaped bacteria such as *Erwinia herbicola* and *Escherichia coli*, an alternate method has been proposed. The model fit in eq 10 for the data on packing spheroids[16] is in reasonable agreement to that presented in Evans and Ferrar for rod shaped bacteria.

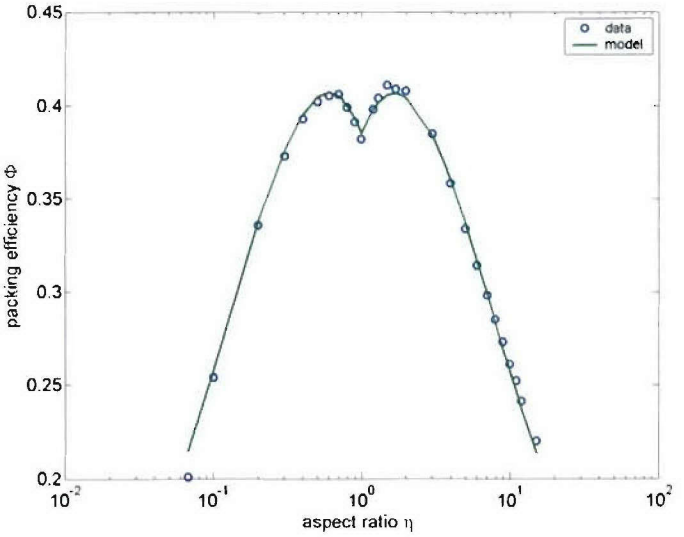

Figure 7. Packing Efficiency as a Function of the Aspect Ratio $\eta = \frac{c}{a}$ of Spheroids (model fit calculated with eq 10).[16]

In Figure 7, packing efficiency as a function of the aspect ratio for packing spheroids is $(\frac{x}{a})^2 + (\frac{y}{a})^2 + (\frac{z}{c})^2 = 1$ (eq 7) with a small aspect ratio, <15. Maximum packing efficiency occurs at $\eta = 1.4$ for a prolate spheroid and $\eta = 0.7$ for an oblate spheroid. The approximate symmetry in the packing efficiency between prolates and oblates $\phi(\eta) \cong \phi(\eta^{-1})$ is clearly shown. A model (polynomial of third order) was fit to the packing efficiency data given as

$$\phi = \left\{ \begin{array}{ll} 0.3849 + 0.0893\ln(\eta) - 0.0999\ln(\eta)^2 + 0.0161\ln(\eta)^3 & 1 \le \eta \le 15 \\ 0.3849 + 0.0893\ln(|\eta|) - 0.0999\ln(|\eta|)^2 + 0.0161\ln(|\eta|)^3 & \frac{1}{15} < \eta < 1 \\ where\ \ \eta = \frac{c}{a} & \end{array} \right\} \qquad (10)$$

The values of the packing efficiency ϕ for bacteria and spores are listed in Table 1.

8. *CL* AND N_{spores} ESTIMATE VIA PACKING EFFICIENCY

The value of the packing efficiency, ϕ, depends on the aspect ratio, η, which is different for a spore (single organism) and a bacterium containing one spore. Therefore, 2 scenarios are addressed for the dissemination of biomaterial:

Scenario I: bacteria (vegetative cells) are disseminated and consequently aggregated to form a size distribution of $f_n(r:\mu,\sigma)$. This scenario is applicable to non-sporulating material such as *E. coli*. Of course, the number of bacteria in the aggregate equals the number of spores. The y-axis is labeled "N_{spores}."

Scenario II: only spores are disseminated and consequently they aggregate to form a size distribution of $f_n(r:\mu,\sigma)$. This scenario is applicable to sporulating material such as Anthrax.

The N_{spores} and *CL* for the 2 scenarios are given as

$$\left\{\begin{array}{l} N_{spores} = \left\{\begin{array}{ll} \dfrac{V\phi(\eta_{bacterium})}{V_{bacterium}} & scenario\ I \\ \dfrac{V\phi(\eta_{spore})}{V_{spore}} & scenario\ II \end{array}\right\} \left(\dfrac{spores}{liter}\right) \\ CL = (N_{spores}10^3) \times (\rho_{spore} V_{spore}) \times L \quad \left(\dfrac{mg}{m^2}\right) \\ V(\mu,\sigma) = \displaystyle\int_{r_{min}}^{r_{max}} \frac{4\pi r^3}{3} f_n(r:\mu,\sigma)dr \ \left(\dfrac{volume\ of\ particles}{liter}\right) \\ N = ACPLA = \displaystyle\int_{r_{min}}^{r_{max}} f_n(r:\mu,\sigma)dr \ \left(\dfrac{particles}{liter}\right) \end{array}\right\} \qquad (11)$$

where ρ_{spore} is the spore density, and V_{spore} and $V_{bacterium}$ are the volume of a single spore and bacterium, respectively (eq 8, Table 1). A single spore mass (Table 1, *mg*) is represented by $\rho_{spore}V_{spore} = m_{spore}$; $N_{spores} \times 10^3$ is the number of spores within a cubic meter $(\frac{spores}{m^3})$; and L is the path-Length (*m*). The effect of the bacterium and spore shape is taken into account when computing the volumes, V_{spore} and $V_{bacterium}$, in eq 8.

In eq 11, a spherical aggregate with a lognormal size distribution, $f_n(r:\mu,\sigma)$, was assumed as given in eq 1, with a total number of aggregates, N, (in a unit volume) and a total volume, $V(\mu,\sigma)$, of the aggregates, shown in Figures 10 and 11.

The N_{spores} for 1 *ACPLA* and corresponding *CL* for a path-Length of 100 *m* are illustrated in Figures 8 to15. The N_{spores} and *CL* for a family of lognormal size distribution $f_n(r:\mu,\sigma)$ in which the spore and bacterium are chosen as *BG* are presented in Table 1. In Figures 8 to 11, the radii range in $f_n(r:\mu,\sigma)$ is $r_{min} \to 0$ and $r_{max} = 25\mu m$. In Figures 12 to 15, $r_{min} \to 0$ and $r_{max} = 5\mu m$ were selected to represent a scenario in which large sized particles are discarded and only small sized particles are present.

When $r_{min} = 0.5\mu m$ in $f_n(r:\mu,\sigma)$, the radius has no agent-containing particles smaller than $0.5\mu m$. The *CL* and N_{spores} computed with eq 11 are higher by 18% because the number of aerosol particles (*N*) were constructed to be the same as when $r_{min} \to 0$. Thus, the size distribution $f_n(r:\mu,\sigma)$ will contain more of the big particles. On the other hand, if $r_{min} \to 0$ is maintained in the size distribution (*N*) in eq 11 but the volume (V) is computed only for $r_{min} \geq 0.5\mu m$, the value for N_{spores} and *CL* will be within 1% of those computed with $r_{min} \to 0$ as shown in Figures 16 to 23.

In Figures 8 and 9, N_{spores} and CL are presented for Scenario I (dissemination of bacteria). In Figures 10 and 11, N_{spores} and CL are shown for Scenario II (dissemination of spores). In Figures 12 to 15, the situation for 1 $ACPLA$ is depicted for a size distribution with only small particles ($r < 5\mu m$). Figures 12 and 13 show the N_{spores} and CL for Scenario I and in Figures 14 and 15, N_{spores} and CL are presented for Scenario II. Figure 11 provides some insight into the crossover of the curves in Figures12 and 13.

Figures 8 and10 show that for $f_n(r:\mu=1,\sigma=2)$ (Fig. 1b), the appropriate N_{spores} for 1 $ACPLA$ is about 3 and 32 for the dissemination of bioaerosols in the form of bacteria (Scenario I) and spores (Scenario II), respectively. The N_{spores} for the dissemination of only spores is much larger (approximately a factor of 10) due to the ratio $[\frac{\phi(\eta_{spore})}{V_{spore}}][\frac{\phi(\eta_{bacteria})}{V_{bacteria}}]^{-1}$ in eq 11. The corresponding CL in Figures 9 and 11 is about 0.11 and 1.2 $\mu g/m^2$, respectively.

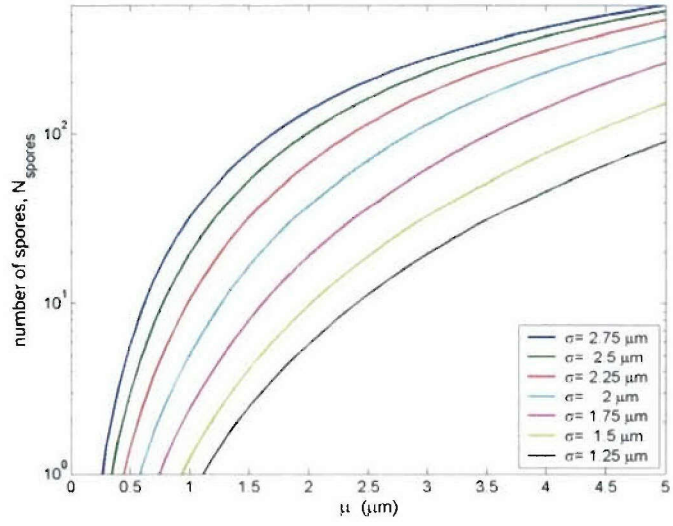

Figure 8. Bacteria or Spore N_{spores} Disseminated as Vegetative Cells (calculated with eq 11 for packing efficiency of BG bacteria).

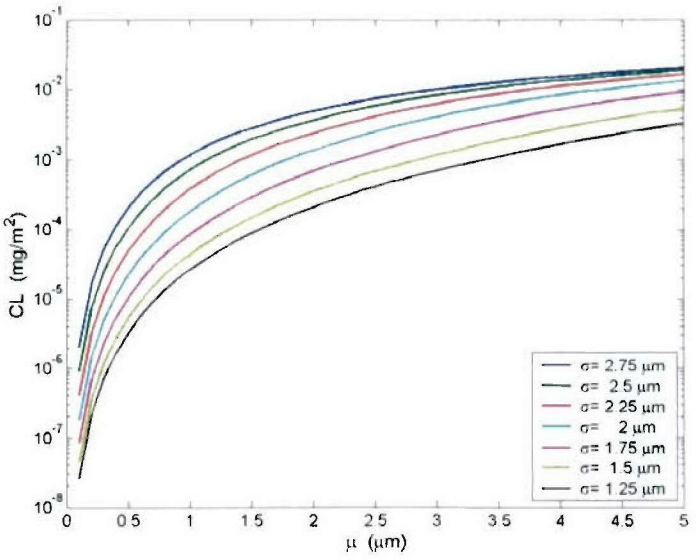

Figure 9. Corresponding *CL* to Bacteria or Spore N_{spores} in Figure 8 (calculated with eq 11 for packing efficiency of *BG* bacteria) (path-Length = 100 m N = ACPLA = 1 l^{-1}).

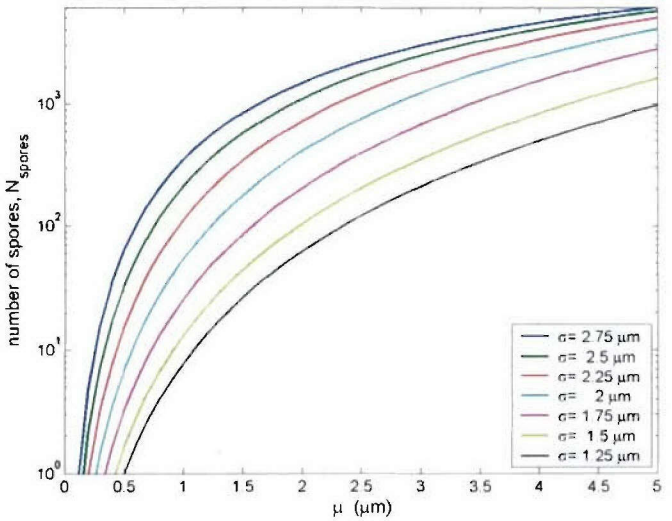

Figure 10. *BG* Bacteria or Spore Count (Table 1) Disseminated as Only Spores (ScenarioII) (calculated with eq 11 for packing efficiency of *BG* bacteria).

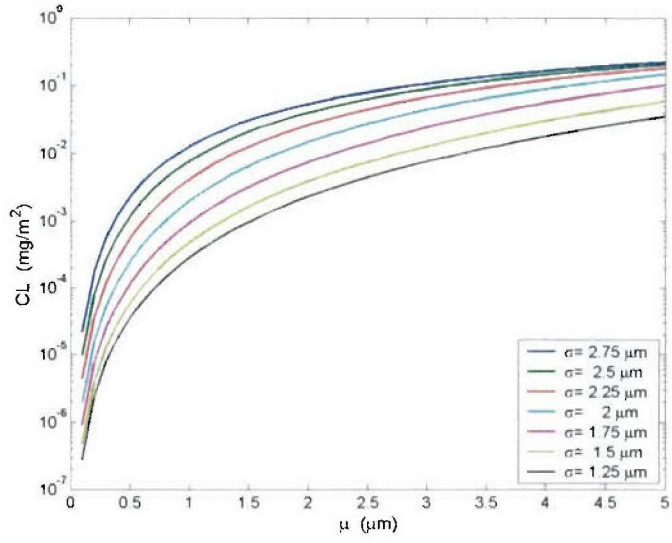

Figure 11. Same as Figure 9 but Calculated for *BG* Spores.

Table 2 displays the values of N_{spores} for *BG* dissemination (Scenario I and II) for 1000 *ACPLA* and the corresponding *CL* values for a path-Length of 100 *m* and size distribution, $f_n(r:\mu=1,\sigma=2)$ ($r<5\mu m$ and $r<25\mu m$). All the values presented in Table 2 can be easily computed with eqs 1, 8, 10, and 11, values from Table 1 (first 2 columns), and volumes from Figures 3 and 4. The estimated *CL* via packing efficiency is smaller than the estimated *CL* in Section 4, where packing efficiency and the shape of the bacteria were not taken into account. The *CL* in Table 2 is also smaller than the estimated *CL* given via the "rule of thumb" discussed in Section 6.

Table 2. Bacteria or Spore Count and *CL* for 100-*m* path-Length of *BG* Bioaerosols Disseminated as Bacteria (Scenario I) and Spores Only (Scenario II).

$ACPLA=1000\ (liter^{-1})$ $L=100\ (m)$ *BG* bacteria and spores	$f_n(r:\mu=1,\sigma=2)$ $0<r<5\mu m$		$f_n(r:\mu=1,\sigma=2)$ $0<r<25\mu m$	
	Scenario I	Scenario II	Scenario I	Scenario II
Number of bacteria or spores $N_{bacteria}, N_{spores}$	3022 (~3 per particle)	32496 (~30 per particle)	4995 (~5 per particle)	53712 (~50 per particle)
Concentration-path-Length $CL\ (\frac{mg}{m^2})$	0.1092 (~0.1 μg/m^2 per particle)	1.174 (~1 μg/m^2 per particle)	0.1805 (~0.2 μg/m^2 per particle)	1.9405 (~2 μg/m^2 per particle)

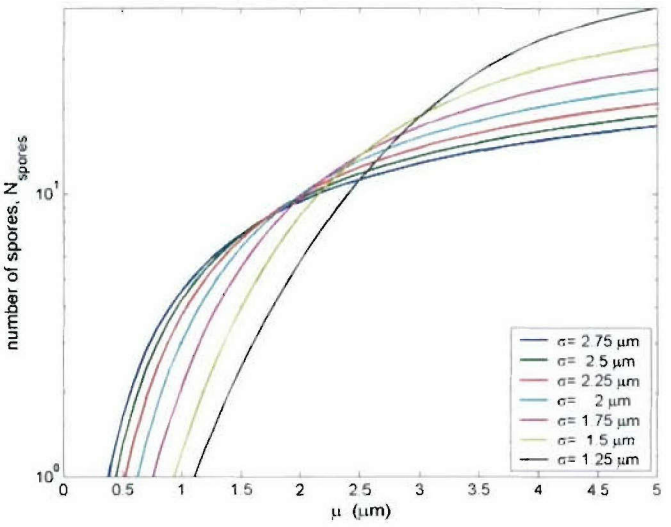

Figure 12. *BG* Bacteria or Spore Count (Table 1) Disseminated as Vegetative Cells (Scenario I) with Small Particle Size Distribution.

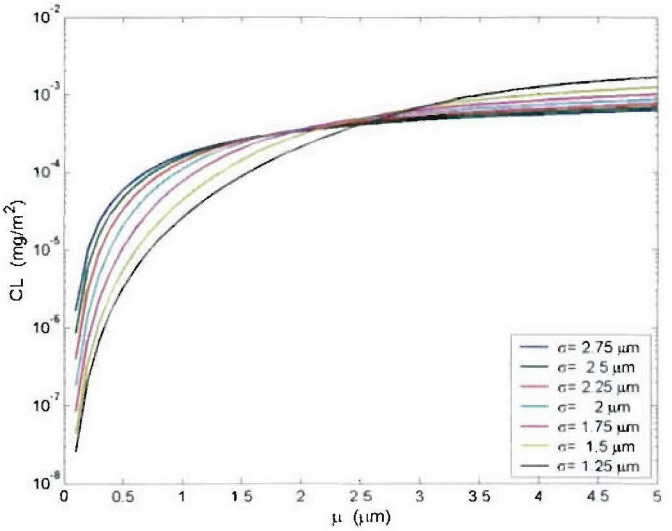

Figure 13. Corresponding *CL* to Bacteria or Spore Count in Figure 12 (Scenario I).

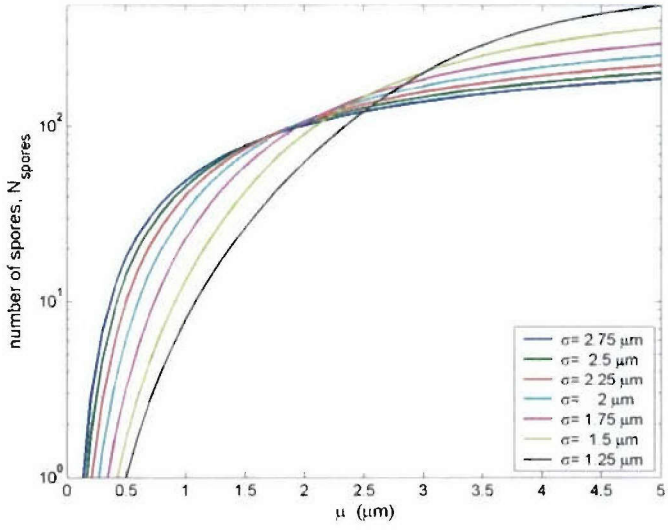

Figure 14. BG N_{spores} (Table 1) Disseminated as Spores (Scenario II) with Small Particles Size Distribution.

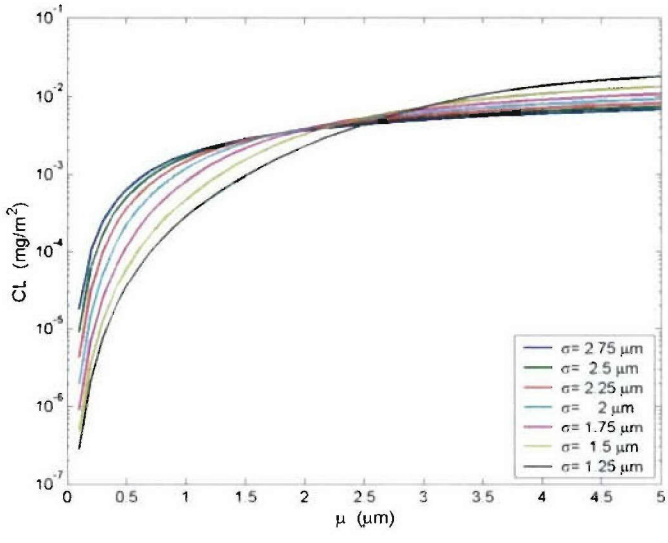

Figure 15. Corresponding *CL* to N_{spores} in Figure 14 (Scenario II) (calculated with eq 11 for packing efficiency of *BG* spores).

9. SUMMARY

The primary objective of this study was to develop relationships and transformations between the number of spores (N_{spores}), Agent-Containing-Particles per Liter of Air (*ACPLA*), and the Concentration-path-Length (*CL*) for aerosols with lognormal size distribution. For the estimation of N_{spores} and *CL*, 2 methods were presented:

(I) The "rule of thumb" (Section 6) in which N_{spores} was taken as the function of the radius of an *ACPLA* aerosol.

(II) Packing efficiency and shape superspheroid for bacteria and spores (Section 8).

For method II, 2 dissemination scenarios were given:

(a) The dissemination and aggregation of bacteria to form a lognormal size distribution $f_n(r:\mu,\sigma)$ of agent-containing aggregates. This scenario is applicable to non-sporulating material (e.g., *Escherichia coli*).

(b) The dissemination and aggregation of only spores to form the lognormal size distribution $f_n(r:\mu,\sigma)$ of aggregates. This scenario is applicable for sporulating material such as Anthrax.

An upper-limit estimate of *CL* (Section 4) was also presented, where *ACPLA* particles were assumed to be entirely composed of spores and packing efficiency was ignored. The relationship between the number of spores and CL is useful for computing fluorescent cross-sections from bioaerosols. For example, if it is known that only a fraction of the spore material (e.g., Tryptophan) is the source of the sought after fluorescence, the *CL* estimate can be adjusted by the fraction of mass due to the material.

The estimate of N_{spores} and *CL* via packing efficiency and their shape was found to be the preferred method. This study has provided numerical examples for N_{spores} and *CL* for 1000 *ACPLAs* and a path-Length of 100 *m* for *BG* bacteria and spores. In the examples, $f_n(r:\mu=1,\sigma=2)$ was selected as the appropriate aerosol size distribution, as this distribution (Fig. 1ab) seems to be a viable representation of *BG Bacillus subtilis* bioaerosols. The different numerical examples are presented in Table 3.

Table 3. *BG* Bacteria and Spore Estimations by 3 Methods of Computation.

$ACPLA = 1000\ liter^{-1}$ with aerosol lognormal size distribution $f_n(r:\mu=1,\sigma=2)$ and a path-Length of 100 *m* of *BG* bioaerosols			N_{spores} $(liter^{-1})$	CL $(\frac{mg}{m^2})$
Estimate via packing efficiency and effect of bacteria and spores shape (Eqs. 8,11)	Scenario I (dissemination of bacteria)	$0 < r < 5\mu m$	3,000	0.11
		$0 < r < 25\mu m$	5,000	0.18
	Scenario II (dissemination of spores)	$0 < r < 5\mu m$	32,500	1.17
		$0 < r < 25\mu m$	54,000	1.94
Estimate via "rule of thumb" (Eq. 9)	$N_{spores}(r) = (2r)^{2.55}$	$0 < r < 5\mu m$	20,000	0.71
		$0 < r < 25\mu m$	30,000	1.07
Upper limit estimate (Eq. 6)	ACPLA aerosols are regarded as spores	$0 < r < 5\mu m$		2.6
		$0 < r < 25\mu m$		5.3

Blank

LITERATURE CITED

1. Ben-David, A. *Particle's Concentration and Size Distribution Downwind on the Ground from an Instantaneous Source.* Presented at the Proceedings of the International Symposium on Spectral Sensing Research, Quebec City, Canada, 10-15 June 2001; pp 79-92.

2. Gurton, K.P.; Ligon D.; Kvavilashvili, R. *Extinction, Absorption, Scattering, and Backscatter for Aerosolized Bacillus Subtilis Var. Niger Endospores from 3 to 13 μm* ; ARL-TR-2343; U.S. Army Research Laboratory: Adelphi, MD, February 2001.

3. Tuminello, P.S.; Arakawa, E.T.; Khare, B.N.; Wrobel, J.M.; Querry M.R.; Milham, M.E. Optical Properties of *Bacillus Subtilis* Spores from 0.2 to 2.5 *μm* . *Appl. Opt.* **1997,** *36*, pp 2818-2824.

4. Dean D.H.; Douthit, H.A. Buoyant Density Heterogeneity in Spores of *Bacillus subtilis*: Biochemical and Physiological Basis. *J. Bacteriol.* **1974,** *117*, pp 601-610.

5. Wyatt, P.J. Differential Light Scattering: A Physical Method for Identifying Living Bacterial Cells. *Appl. Opt.* **1968,** *7*, pp 1879-1896.

6. Wriedt, T. Using the T-matrix Method for Light Scattering Computations by Non-Axisymmetric Particles: Superellipsoids and Realistically Shaped Particles. *Part. Syst. Charact.* **2002,** *19*, pp 256-268.

7. Santo, L.Y.; Dori, R.H. Ultrastructural Analysis during Germination and Outgrowth of *Bacillus subtilis* Spores. *J. Bacteriol.* **1974,** *120*, pp 475-481.

8. Weber, P.; Greenberg, J.M. Can Spores Survive in Interstellar Space? *Nature* **1985,** *316*, pp 403-407.

9. Munakata, N.; Hieda, K.; Kobayashi, K.; Ito, A.; Ito, T. Action Spectra in Ultraviolet Wavelengths (150-250nm) for Inactivation and Mutagenesis of *Bacillus-subtilus* Spores Obtained with Synchrotron Radiation. *Photochem. Photobiol.* **1985,** *44*, pp 385-390.

10. Salzman, G.C.; Singham, S.B.; Johnston, R.G.; Boohren, C.F. Light Scattering and Cytometry. In *Flow Cytometry and Sorting*; Melamod, M., Lindino, T., Mendelsohn, M.L., Eds.; Wiley-Lis: New York, 1990; pp 81-107.

11. Bronk, B.V.; Druger, S.D.; Czege, J.; Van De Merwe, W.P. Measuring Diameters of Rod-Shaped Bacteria in Vivo with Polarized Light Scattering. *Biophys. J.* **1995,** *69*, pp 1170-1177.

12. Arakawa, E.T.; Tuminello, P.S.; Khare, B.N.; Milham, M.E. Optical Properties of *Erwinia herbicola* Bacteria at 0.190-2.50 μm. *Biopolymers Biospectroscopy* **2003,** *72 (5)*, pp 391-398.

13. Wolfram, S. http://mathworld.wolfram.com/SpherePacking.html (accessed Jan-June 2001).

14. Sloane, N.J. http://www.research.att.com/~njas/ (accessed Jan-June 2001).

15. Williams, S.R.; Philipse, A.P. Random Packing of Spheres and Spherocylinders Simulated by Mechanical Contraction. *Phys. Rev.* **2003,** *E67*, 051301, pp 1-9.

16. Sherwood, J.D. Packing of Spheroids in Three-Dimensional Space by Random Dequential Addition. *J. Phys.* **1997,** *A, 30*, pp 839-843.

17. Evans, K. E.; Ferra, M.D. The Packing of Thick Fibers. *J. Phys.* **1989,** *D 22*, pp 354-360.

18. Faris, G.W.; Copeland, R.A.; Mortelmans, K.; Bronk, B.V. Spectrally Resolved Absolute Fluorescence Cross-Sections for *Bacillus* Spores. *Appl. Opt.* **1997,** *36*, pp 958-967.

DEPARTMENT OF THE ARMY
CDR USARDECOM
ATTN AMSRD CII
5183 BLACKHAWK ROAD
APG MD 21010-5424

OFFICIAL BUSINESS

FIRST CLASS